NEUTRON MEASUREMENTS WITH ^{4}He SiPM GAS SCINTILLATION DETECTORS IN HIGH GAMMA ENVIRONMENTS

S. S. Gokhale[a], R. P. Kelley[a], T. Zhu[a], Y. Liang[a], H. Chung[b], S. Kiff[c], R. Chandra[d], H. Ray[a], A. Enqvist[a], and K. A. Jordan[a]

[a] *University of Florida, Nuclear Engineering Program, Gainesville, FL 32611-6400, United States*
[b] *Korea Atomic Energy Research Institute, Daejeon, 305-353 Korea*
[c] *Sandia National Laboratories, California, P.O. Box 969, CA 94551,0969, United States*
[d] *Arktis Radiation Detectors Ltd., Räffelstrasse 11, 8045 Zürich, Switzerland*

Abstract

The goal of this investigation was to evaluate the capability of the ^{4}He gas scintillation detectors to unambiguously detect neutrons when exposed to a high gamma-ray intensity environment. This neutron-gamma discrimination capability of the detectors is vital for applications such as spent nuclear fuel monitoring. A 315 Ci ^{137}Cs gamma-ray source was used to simulate the high gamma environment produced by a spent fuel storage cask. The gamma flux incident on the detector was varied by adjusting the position of the source within its shielded housing. A 1 Ci PuBe neutron source was introduced to evaluate capability of the detectors to differentiate neutron events in the presence of the high gamma flux.

1. Introduction

Recently, the development of techniques and technologies for spent nuclear fuel assay has been the subject of great interest for international safeguards [1][2]. The radiation detection systems traditionally used for these applications rely on thermal neutron detectors or liquid scintillator detectors. Thermal neutron detectors such as ^{3}He and BF_3 gas detectors have high counting efficiency, however they do not provide incident neutron energy information. Liquid scintillators on the other hand are capable of providing neutron energy information, however they are more sensitive to gamma-ray interactions and cannot easily differentiate between gamma-ray and neutron interactions which is critical for many neutron detection applications [3]. Pulse shape discrimination (PSD) techniques have been successfully applied to separate the detector output caused by neutron and gamma-rays [4][5], however the capability of liquid scintillators to provide neutron energy information is limited due to internal moderation and multiple scattering interactions within the detector [6].

The ^{4}He fast neutron scintillation detector, developed by Arktis Radiation Detectors Ltd., is a relatively new tool and has several advantages over traditional thermal neutron detectors and liquid scintillators. ^{4}He is naturally abundant and readily available compared to ^{3}He. The ability of the ^{4}He gas scintillation detectors to be used for fast neutron detection applications such as fissile material detection and active neutron interrogation has been demonstrated in the past[7][8]. ^{4}He has a high elastic scattering cross section at fast neutron energies, particularly the cross section has a resonance peak around 1 MeV which matches the peak emission of fission neutrons. Since the neutrons do not need to be moderated in order to be detected, the neutron energy information is preserved Additionally, because of the low electron density of ^4He the detectors have very low sensitivity to gamma-rays and hence have excellent gamma rejection [9][10].

In this work we investigated the neutron detection capability of the Arktis ^4He SiPM detectors in a high gamma-ray environment. The purpose of this investigation was to determine the feasibility of the ^4He SiPM detectors of both extended (XR) and non-extended range (NXR) detectors to be used for spent nuclear fuel monitoring. It was observed that the ^4He SiPM detectors performed well compared to other scintillator detectors that have been studied for similar applications in the past [11][12][13].

2. Experimental Setup

a. ^{4}He SiPM Detector

The next generation of ^4He fast neutron detectors developed by Arktis Radiation Detectors uses silicon photomultipliers (SiPM) to detect the light produced by helium gas scintillation. The detectors show great potential to be used for special nuclear material (SNM) detection and spent nuclear fuel (SNF) measurements. A schematic of the new SiPM detectors can be seen in Fig. 1. In the old models, the photomultiplier tubes (PMTs) were located on either end of the detector tube, which limited the size of the active detector volume. With the SiPM light detection technology embedded directly along the central axis of the detector, almost all of the volume is active fill gas that is eligible for neutron detection. The introduction of SiPMs also removes some of the sensitivities associated with PMTs, making this new generation of detectors immune to shock, vibration, and magnetic fields.

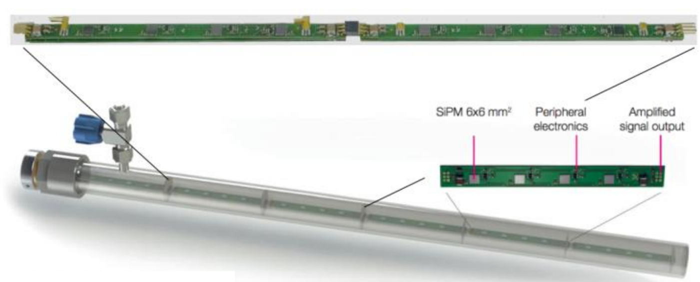

Figure 1. Schematic of the new Arktis extended range ^4He detector.

In addition to replacing PMTs with SiPMs for light collection, the next generation of Arktis neutron detectors also offers an extended energy range variant that is able to detect thermal neutrons, through the addition of a coating of a ^6Li compound on the inside of the detector tube. This extended range design allows for simultaneous detection of thermal neutrons, fast neutrons, and gamma-rays, which can be analyzed together to provide much more information about a measured source and any intermediary shielding.

The baseline Arktis detector has an active volume of ~6 cm diameter and ~60 cm length. The steel cylinder is filled with ^4He gas compressed at a pressure of 180 bar. Scintillating UV light resulting from neutrons interacting with the ^4He is converted into blue (420 nm) light by a wavelength shifting material coated on the inside of the cylinder. The scintillation photons are collected by the SiPMs. The SiPMs are mounted along the central axis of the detector in order to have improved light collection since it requires fewer reflections to convey the scintillation photons onto the sensitive surface [14].

Each segment of the detector contains four pairs of SiPMs. The output signals of each SiPM pair are summed and fed into a single output channel. Time over Threshold (ToT) is the calculated segmentwise using the signals of all SiPMs. To calculate the ToT value, each signal of a SiPM pair is fed into a discriminator. If the signal is above the offset threshold, the input line corresponding the SiPM pair into the coincidence unit is set to high. If two input signals are set to high within 30 ns, the ToT calculation counter is incremented. The neutron/gamma and the fast/thermal neutron discrimination is based on this ToT parameter. The ToT parameter represents the time for which the amplitude of the output pulses of the detector are above a configurable threshold. As described above, the ToT is calculated segmentwise using the signals from all the SiPMs. The ToT value is compared to preconfigured cuts that were determined experimentally and the output pulses are binned accordingly to produce a histogram.

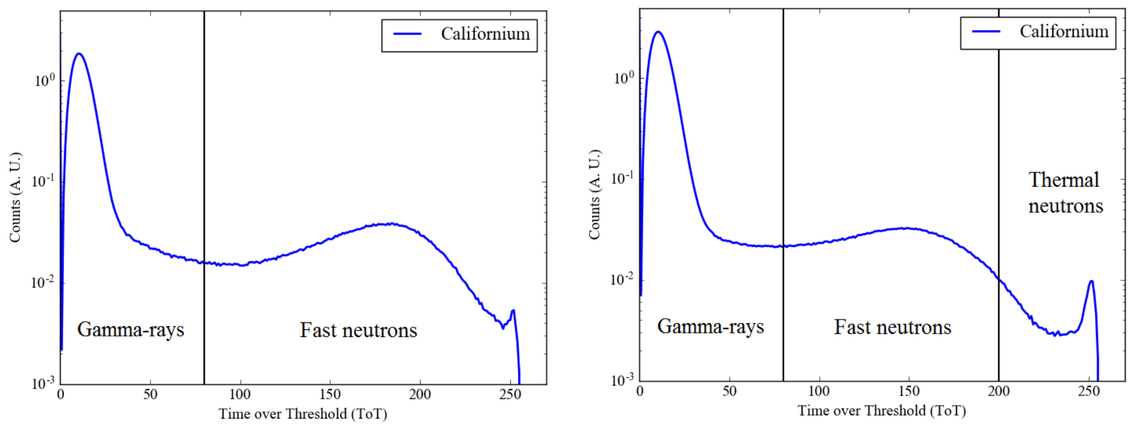

A B

Figure 2. ToT histograms of ^{252}Cf neutron spectra produced using ^{4}He SiPM detectors of, A) non-extended range (NXR), and B) extended range (XR). The vertical lines indicate the cuts that differentiate the gamma/fast neutron/thermal neutron events.

Figure 2. shows the ToT histograms produced by irradiating the ^{4}He SiPM detectors with neutrons and gamma-rays from a ^{252}Cf neutron source. The histograms are divided into different regions based on the different cuts applied to the ToT pulses. Figure 2A. shows the ToT histogram for the NXR detector, while figure 2B is for the XR detector. The ToT of the output pulses due to gamma-ray interactions is smaller than that of the neutron pulses, therefore gamma-ray pulses are binned in the lower ToT channels. In the case of the XR detector, the output pulses produced by the thermal neutrons in the $^{6}Li(n,\alpha)$ reaction have larger ToT than the pulses due to the elastic scattering interaction of the fast neutrons with the ^{4}He gas. As a result, the thermal neutron pulses are binned in the highest ToT channels.

b. High Gamma Environment

The University of Florida ^{137}Cs Calibration Facility was used as a high-gamma environment to simulate the radiation from spent nuclear fuel. The 315 Ci ^{137}Cs source is kept underground in a well with a shielded collimator. The gamma ray flux at the collimator entrance can be varied by repositioning the source vertically in the source well using a pulley system. Lead drawers can also be removed or inserted as necessary to further adjust the gamma-ray flux. A schematic of the source assembly can be seen in figure 3.

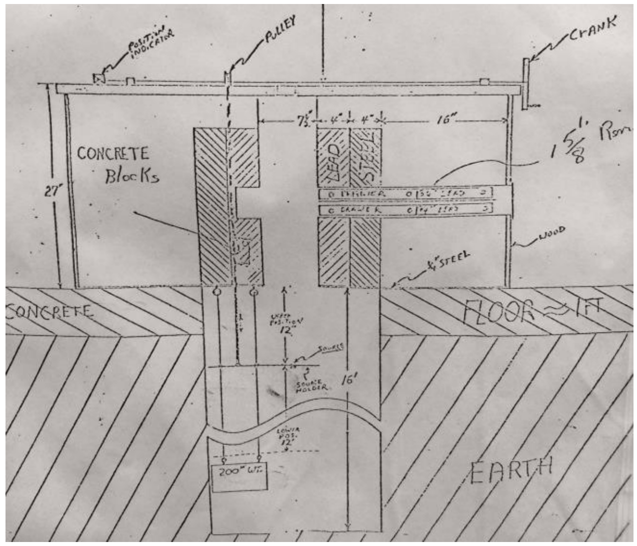

Figure 3. Schematic of the source geometry at the University of Florida ^{137}Cs calibration facility.

For the measurements, the detector tube was laid over the opening to the source well. The source was elevated up and down to different positions in order to vary the gamma flux incident on the detector. The source was adjusted to 20 different positions, where a higher position indicates that the source is farther from the detector and thus the exposure rate is lower. In addition to the high gamma flux from the ^{137}Cs source, a 1 Ci PuBe source was added at different measurement points in order to evaluate how well the detector could differentiate neutron events in the presence of a high gamma flux. Table 1. shows the gamma-ray flux values at the collimator opening corresponding to the different source positions.

Table 1. gamma-ray exposure rate at collimator entrance for different source positions

Position	Exposure Rate (mR/hr) Bottom drawer open	Exposure rate (mR/hr) Both drawers open
20	15	465
15	22	681
10	39	1144
5	83	2387
0	318	8160

The combined ^{137}Cs and PuBe source configuration provides an approximate analog to the gamma-ray and neutron environment that the detectors would be exposed to in spent nuclear fuel monitoring applications. Previous studies have shown that for a typical high burn-up spent fuel rod from a light water reactor (LWR) the neutron and gamma-ray emission rates are in the range of 3E6 – 9E6 neutrons/second and 1.5E9 – 1.7E9 gammas/second respectively [15].

3. Results

The segmentwise time over threshold histograms recorded at different gamma-ray exposure rates for an XR detector can be seen in figure 4. Each subplot/pane represents the response of a segment of the detector and shows six ToT histograms recorded at different ^{137}Cs source positions. Two measurements were conducted at the source position corresponding to an exposure rate of 318 mR/hr, where the second measurement included the introduction of the PuBe neutron source. Each measurement was carried out for an acquisition time of 5 minutes.

The position of the detector over the source well effectively collimated the gamma-rays onto the middle segment, which explains the lower number of gamma-ray counts in the two side segments. From the figure it can be seen that each source position can be distinguished by a change in the height of the gamma peak. The introduction of the PuBe source (yellow) does not appreciably change the height of the gamma peak, however it causes a clear shift in the number of counts in the fast and thermal neutron regions. The neutron events can be clearly distinguished from the gamma-rays, even when the detector is exposed to this high gamma-ray exposure rate.

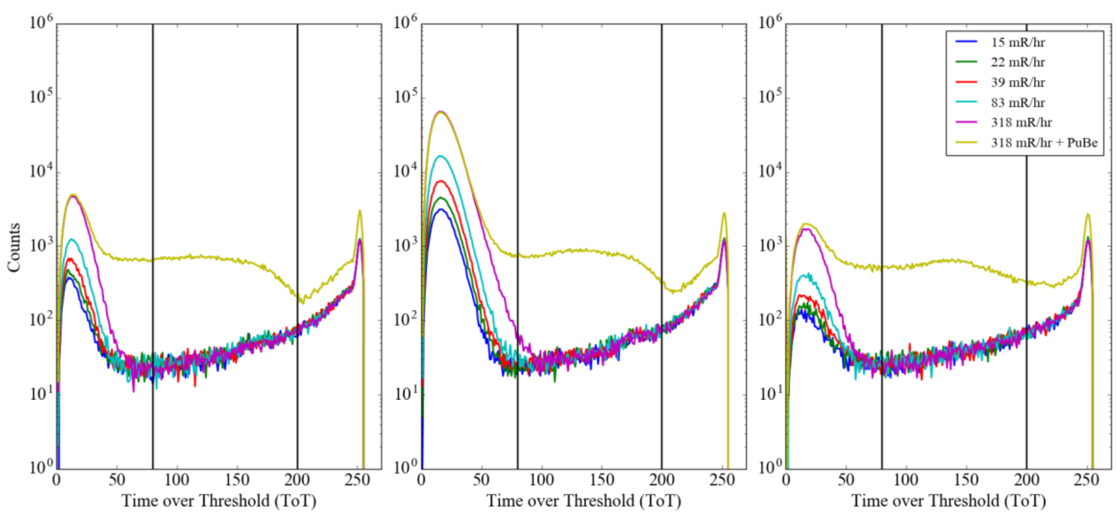

Figure 4. Segmentwise output of the ^{4}He SiPM XR detector. The introduction of the PuBe source does not appreciably change the gamma portion of the response, but can be seen to cause a distinct change in both neutron regions.

It is possible that some gamma-ray events may produce pulses with ToT that is sufficient to be misclassified as neutron events and may contribute to the counts in the higher ToT channels. Conversely, some neutron events that undergo partial energy deposition may produce smaller ToT pulses that get discriminated as gamma-ray events. However, from figure 4 it can be seen that the increase in the gamma-ray flux only increases the counts in the "gamma-ray" region of the ToT histograms and the introduction of the PuBe source has a larger effect on the counts in the higher ToT channels.

Integrating the total counts in the different regions of the ToT histograms gives the total number of gamma-rays and neutrons detected at each source position. In the absence of a neutron source, the counts recorded in the fast and thermal neutron regions may be due to a combination of electronic noise, gamma-ray events misclassified as neutrons, and background radiation. As can be seen from figure 5, the total number of counts in the fast and thermal neutron regions remains constant for the different gamma-ray source positions. The number of neutron counts only increases when the PuBe source is introduced. As the gamma-ray exposure rate is increased, the number of counts in the gamma-ray region of the histogram do increase. This is reflected in figure 4 as a broadening of the gamma-ray peak. This broadening may be caused due to pulse pileup due to the increased count rate, which may result in some of the gamma-ray pulses attaining a lager ToT and as a result they are binned in the higher ToT channels. However, it can be seen that at a gamma-ray exposure rate up to 318 mR/hr the number of ToT pulses that may be misclassified as neutron events is not significant.

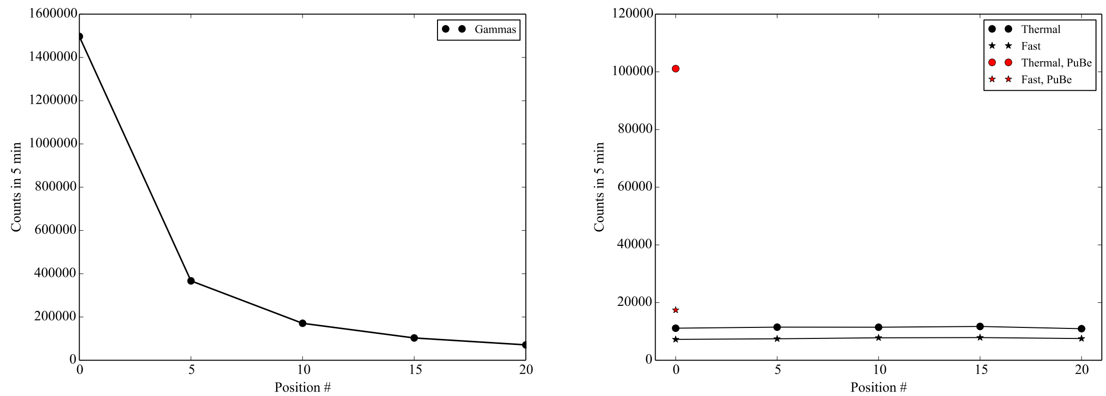

Figure 5. The total number of counts recorded in the different regions of the ToT histograms. The total integrated counts in the gamma-ray region increases with an increase in exposure rate, while the integrated counts in the fast and thermal neutron region remains constant.

As the gamma-ray exposure rate is further increased beyond 318 mR/hr, it can be seen (figure 6) that the gamma peak broadens further and eventually overlaps into the fast neutron region of the ToT histogram. Thus, the ability of the detectors to differentiate between gamma-rays and neutrons reduces as the gamma-ray exposure rate is increased above 318 mR/hr. Finally, as can be seen from figure 6, at an exposure rate of 8160 mR/hr the gamma-ray peak extends completely across the fast neutron region and partially into the thermal neutron region. The introduction of the PuBe source at this exposure rate does cause a change in the number of counts, however due to the pulse pileup the neutrons may not be differentiated from the gamma-ray events unambiguously.

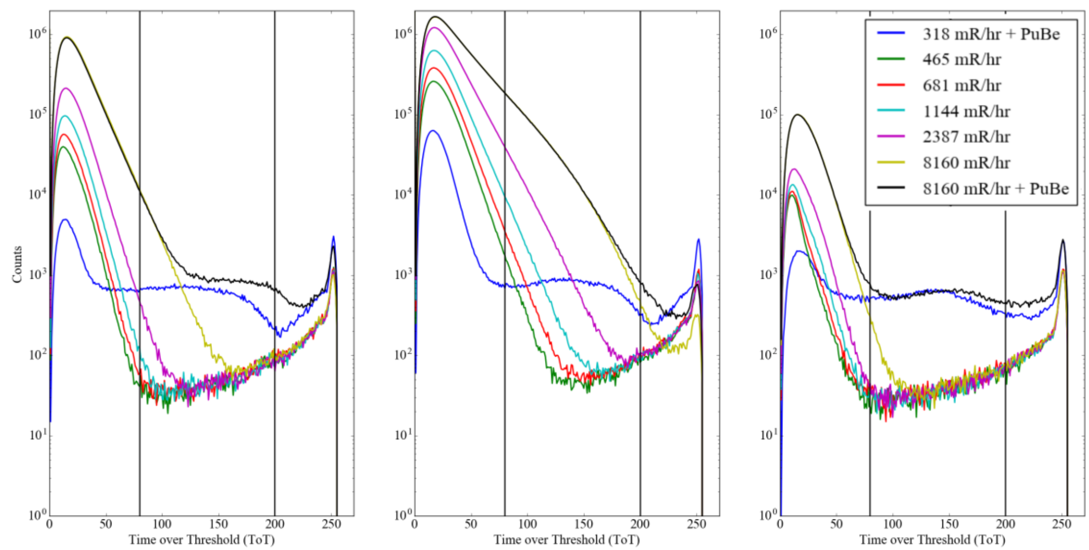

Figure 6. Segmentwise output of the ^{4}He SiPM XR detector at gamma-ray exposure rates greater than 318 mR/hr.

Similar ToT histograms were generated by irradiating the non-extended range ^{4}He SiPM detector at the different gamma-ray exposure rates. The NXR detector exhibited a response similar to the XR detector in the high intensity gamma-ray environment. As can be seen from figure 7, the detector can unambiguously differentiate between gamma-rays and neutrons up to a gamma-ray exposure rate of 318 mR/hr. At gamma-ray exposure rates beyond 318 mR/hr the detector exhibited similar reduction in neutron discrimination ability due to signal saturation and pulse pileup.

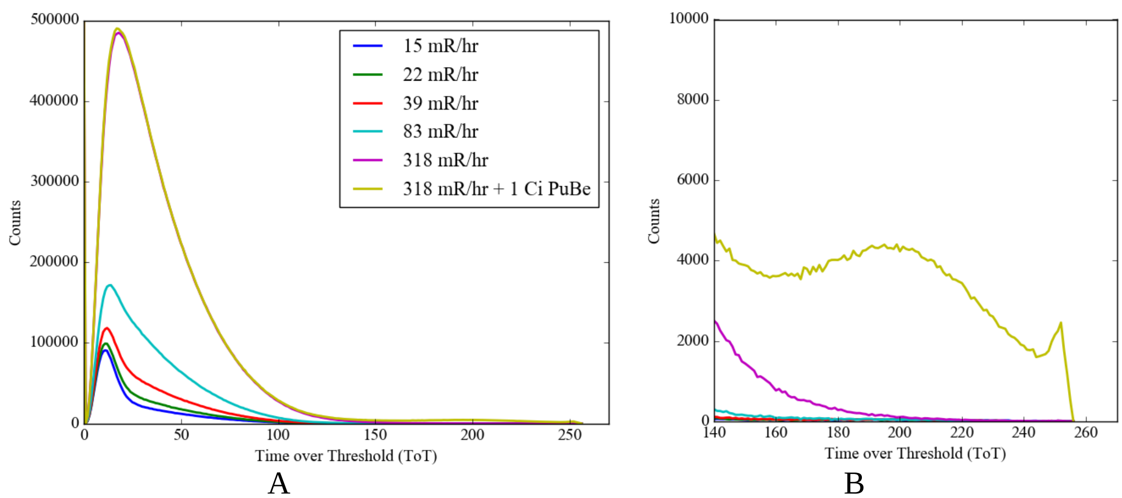

Figure 7. ToT histograms generated using the NXR ^{4}He SiPM detector, while the detector was irradiated at different gamma-ray exposure rates.

4. Summary

These preliminary results illustrate the ability of the new extended range Arktis neutron detectors to simultaneously measure and distinguish between gammas, thermal neutrons, and fast neutrons, and the ability of these detectors to perform this discrimination even in high count rate environments, such as those in the vicinity of a spent fuel cask.

Using the 315 Ci ^{137}Cs source to simulate the high-gamma environment produced by a spent fuel storage cask at the UF ^{137}Cs Calibration Facility, measurements were conducted with an extended range (thermal and fast neutron) and non-extended range (fast neutron only) ^{4}He gas scintillation detectors. In the midst of the high-gamma environment provided by this source, a PuBe neutron source was also introduced to evaluate how well the detector could differentiate neutron events in the presence of a high gamma flux, as would be required for spent fuel measurements. The gamma flux at the detector was varied by adjusting the source position within its shielded housing, while the neutron flux from the PuBe source was held constant in order to determine the maximum gamma levels at which the detector could continue to accurately resolve neutron events.

It was observed that the 1 Ci (20 mR/hr) PuBe source was easily distinguished in the 350 mR/hr gamma background. The results not only illustrate the ability of the new extended range ^{4}He detectors to simultaneously measure and distinguish between gammas, thermal neutrons, and fast neutrons, but specifically demonstrate the ability of these detectors to perform this discrimination even in high count rate environments. These results show promise for the implementation of these new detectors as a new spent fuel measurement tool, with applications to arms control, treaty verification, and the detection of diverted nuclear material from dry storage casks.

5. Reference

[1] S. J. Tobin, H. O. Menlove, M. T. Swinhoe, M. A. Schear, Next generation safeguards initiative research to determine the Pu mass in spent fuel assemblies: purpose, approach, constraints, implementation, and calibration, Nucl. Instr. Meth. A. 652 (2011) 73.

[2] A. V. Mozin, S. J. Tobin, L. W. Campbell, J. R. Cheatham, C. R. Freeman, C. J. Gesh, Determining plutonium mass in spent fuel with nondestructive assay techniques NGSI research overview and update on NDA techniques, Lawrence Berkeley National Laboratory, LBNL paper LBNL-5174E, Available from: http://escholarship.org/uc/item/8df350x5, 2012.

[3] A. Enqvist, I. Pazsit, Calculation of the light pulse distribution induced by fast neutrons in organic scintillation detectors, Nucl. Instr. Meth. A. 618 (2010) 266.

[4] H. Klein, S. Neumann, Neutron and photon spectrometry with liquid scintillation detectors in mixed fields, Nucl. Instr. Meth. A. 476 (2002) 132.

[5] A. Enqvist, C. C. Lawrence, B. M. Wieger, S. A. Pozzi, T. N. Massey, Neutron light output response and resolution functions in EJ-309 liquid scintillation detectors, Nucl. Instr. Meth. A. 715 (2013) 79.

[6] S. A. Pozzi, M. Flaska, A. Enqvist, I. Pazsit, Monte carlo and analytical models of neutron detection with organic scintillation detectors, Nucl. Instr. Meth. A. 582 (2007) 629.
[7] J. M. Lewis, R. P. Kelley, D. Murer, and K. A. Jordan, Fission signal detection using helium-4 gas fast neutron scintillation detectors: theory and experiment, Appl. Phys. Lett. 105 (2014) 1.
[8] D. Murer, R. Chandra, G. Davatz, H. Friederich, U. Gendotti, A. Howard, R. Lanza, P. Peerani, A. Tomanin, ^{4}He detectors for mixed oxide (MOX) fuel measurements, IEEE Nucl. Sci. Conf. R. HE2-3 (2011) 4858.
[9] J. M. Lewis, D. Raetz, D. Murer, and K. A. Jordan, Analysis for in-situ fission rate measurements using ^{4}He gas scintillation detectors, IEEE Trans. Nucl. Sci. 61 (2014)
[10] R. Chandra, G. Davatz, H. Friederich, U. Gendotti,, and D. Murer, Fast neutron detection with pressurized ^{4}He scintillation detectors, J. Inst. 7 (2012) C03035
[11] L. Stevanato, D. Cester, G. Nebbia, G. Viesti, Neutron detection in high gamma-ray background with EJ-301 and EJ-309 liquid scintillators, Nucl. Instr. Meth. A. 690 (2012) 96.
[12] M. M. Bourne, S. D. Clarke, N. Adamowicz, S. A. pozzi, N. Zaitseva, L. Carman, Neutron detection in a high-gamma field using solution-grown stilbene, Nucl. Instr. Meth. A. 806 (2016) 348.
[13] A. C. Kaplan, M. Flaska, A. Enqvist, J. L. Dolan, S. A. Pozzi, EJ-309 pulse shape discrimination performance with a high gamma-ray-to-neutron ratio and low threshold, Nucl. Instr. Meth. A. 729 (2013) 463.
[14] M. Caccia, V. Chmill, A. Martemiyanov, R. Santoro, R. Chandra, G. Davatz, U. Gendotti, Silicon photomultiplier readout of a scintillating noble gas detector for homeland security, IEEE ANIMMA Conf. (2013) 1.
[15] A. Sasahara, T. Matsumura, G. Nicolaou, D. Papaioannou, Neutron and gamma ray source evaluation of LWR high burn-up UO_2 and MOX spent fuels, J. Nucl. Sci. Technol. 4 (2004) 448.